Supporting Information

Fazlollahi et al. 10.1073/pnas.1517140113

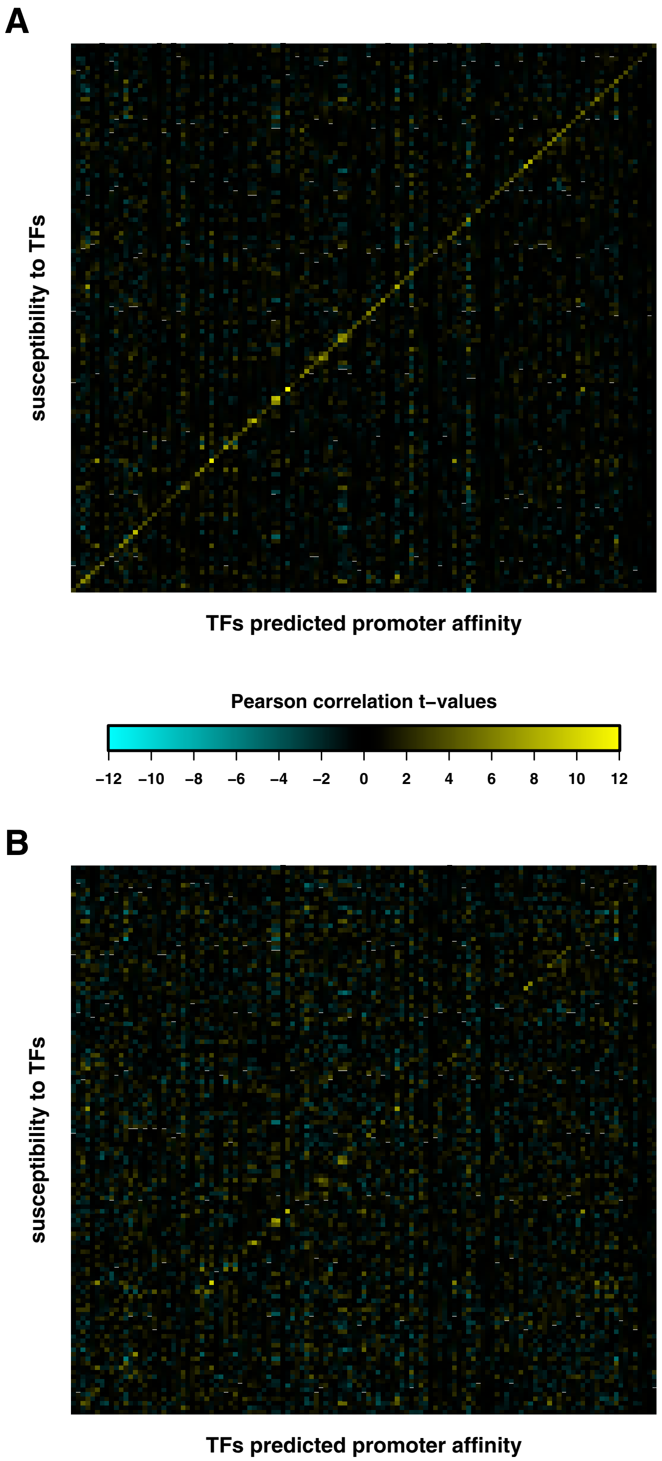

Fig. S1. Resolving the circularity problem for susceptibility calculation. The heat maps summarize *t* values of the Pearson correlation between the susceptibility signatures and promoter affinity profiles for each of the 123 different TFs. For each segregant, first the differential TF activities were obtained by applying multiple regression of differential mRNA abundance of (*A*) all genes and (*B*) all genes but leaving out one gene (*g*) at a time on the TF affinity score profiles. Next, the susceptibilities of each gene (*g*) were obtained by applying multiple regression of the differential mRNA abundance of *g* on the TF activities from *A* and *B*, separately. In *B* the TFs with significant *t* values on the diagonal correspond to the 12 TFs that pass the TF selection step for multiple regression (*Results* and *Materials and Methods*).

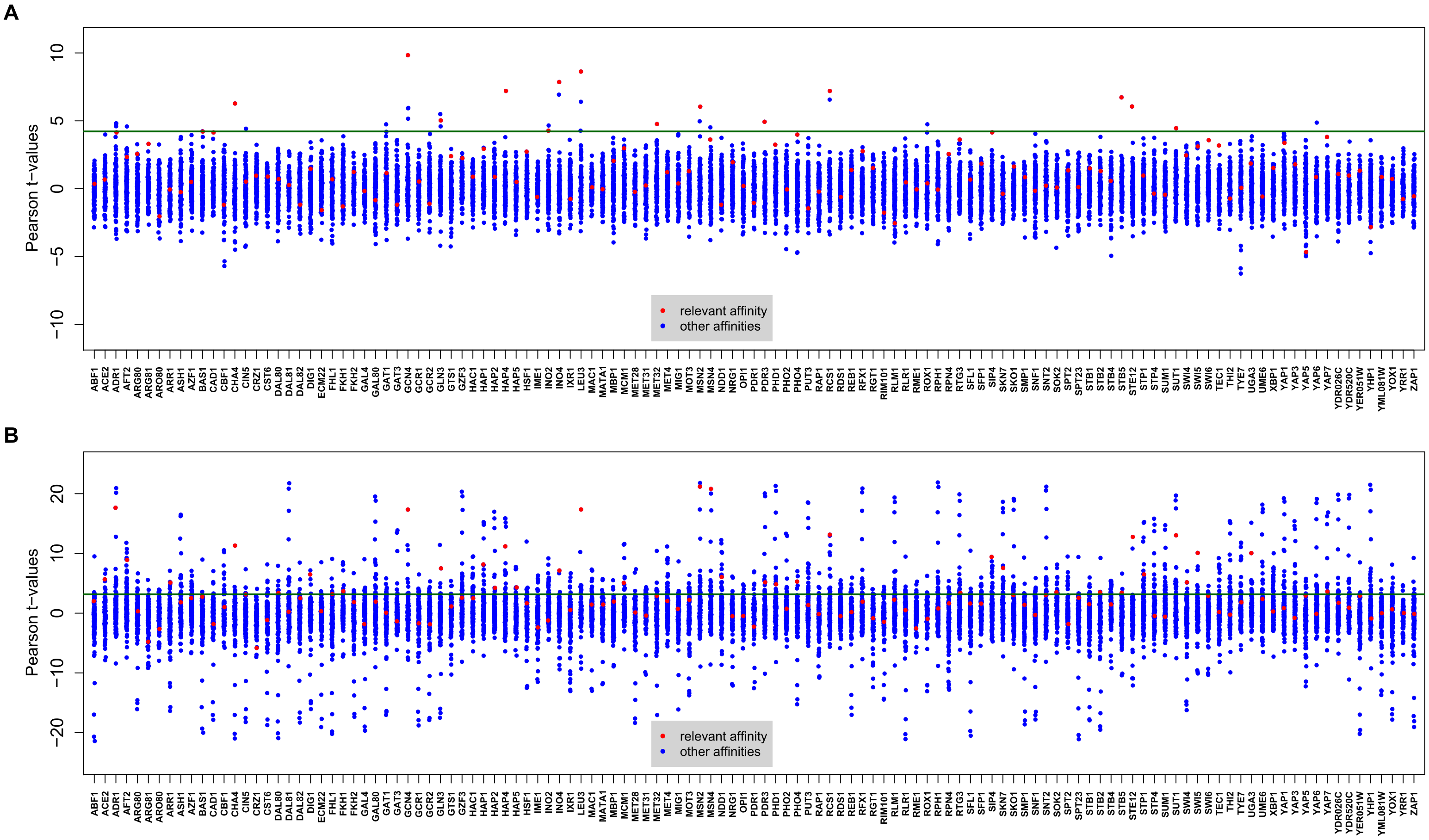

Fig. S2. Correlation between TF susceptibility signatures and promoter affinity profiles (TF acceptance criteria). The susceptibilities were derived using (*A*) multiple regression and (*B*) univariate regression of gene expression on TF activities. The *x* axes in both panels represent the TF for which the susceptibility signature was calculated. For each TF, the *t* value of the correlation of its susceptibility signature to promoter affinity profile obtained from its PSAM (relevant affinity) is pointed out with red dot and to the rest of 122 TFs affinity profile with blue dots. We accepted the TFs whose susceptibility signature (*i*) correlated significantly to their affinity profile (red dots for each column) and (*ii*) this correlation corresponded to the highest Pearson *t* value (i.e., the red dot stands out from the rest of blue dots for each column). The dark green line represents the significant *t*-value threshold at a 1% FDR level. In the case of Msn2p, the correlation was most strongly to Msn4p affinity. However, Msn2p and Msn4p are known to be involved in stress response activation by binding to promoter genes containing a stress response element and can partially compensate for each other's function (64, 65). Therefore, we accepted Msn2p in the selection step.

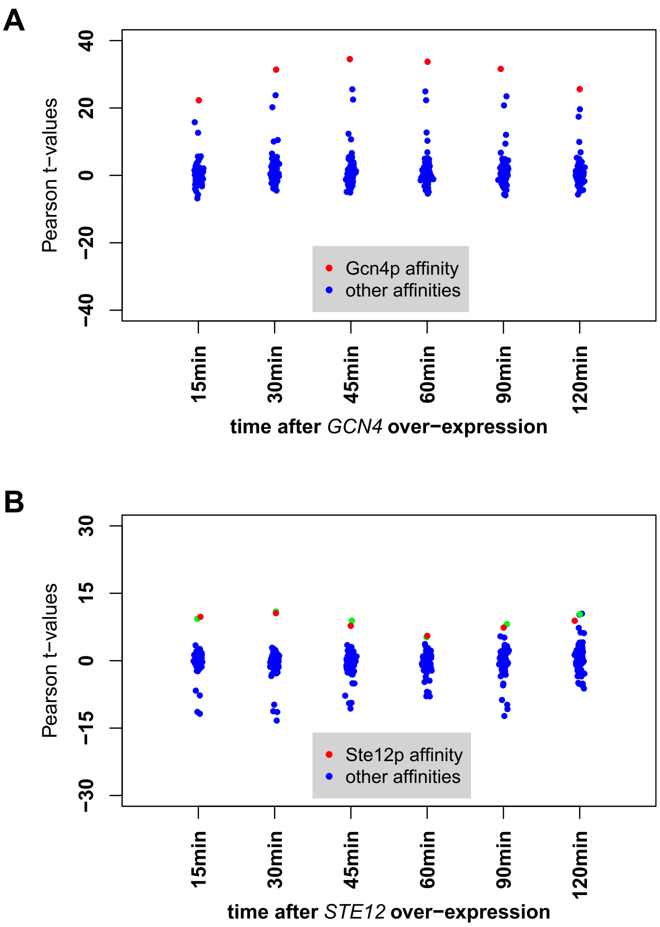

Fig. S3. Correlation between expression response after overexpression of *GCN4* and *STE12* and promoter affinity. The *x* axes represent the overexpression data at different time points. Each point corresponds to the Pearson *t* value of the correlation between the affinity profile of a particular TF and the genome-wide differential mRNA abundance for the overexpression of *GCN4* (*A*) and *STE12* (*B*). The *t* values of the correlation between the affinity profile to Gcn4p, and Ste12p are indicated in red in each relevant panel. Affinity profiles of these two TFs are exclusively correlated with the overexpression data. The green dots in *B* correspond to Dig1p, a known cofactor of Ste12p (21). These results demonstrate that the in vitro occupancies correlate significantly to the in vivo function of Gcn4p and Ste12p.

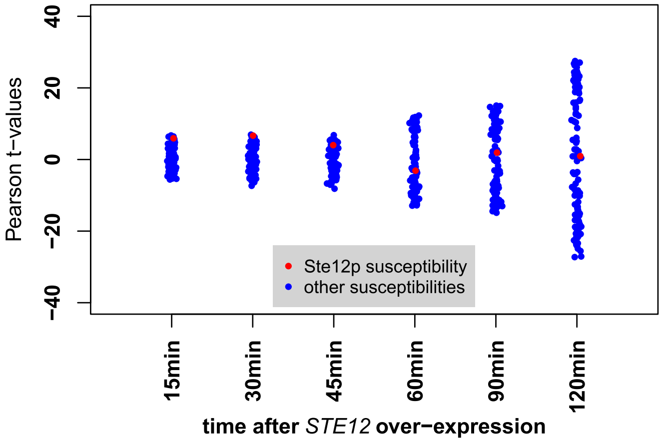

Fig. S4. Correlation between expression response to *STE12* overexpression and regulatory susceptibility. The *x* axis represents the overexpression data at different time points. Each point corresponds to the Pearson *t* value of the correlation between the susceptibility signature for a particular TF and the differential mRNA abundance in the overexpression experiment. The *t* values of the correlation to susceptibility signature for Ste12p are indicated in red in each time point column. For Ste12p, the correlation is not significant from the 30-min time point onwards (*Results*).

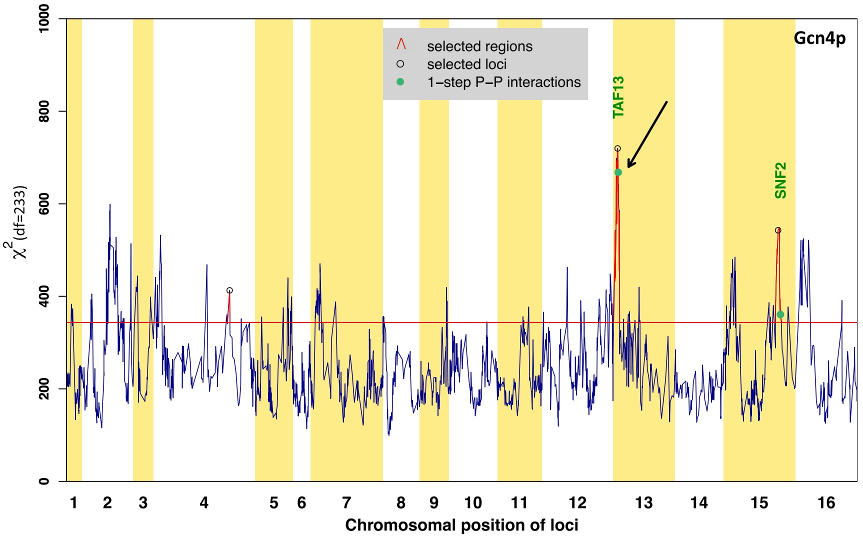

Fig. S5. χ^2 statistic profile obtained for Gcn4p. The analysis was performed using positive targets of Gcn4p (233 genes). We performed forward selection to detect peaks at a Bonferroni-corrected *P* value <0.01. The selected loci are marked with black circles. Green dots indicate the location of genes within the significant cQTL regions whose encoded protein has a direct physical interaction with Gcn4p. The horizontal red line represents the χ^2 statistic significant threshold at 1% level with Bonferroni correction. The black arrow indicates the *TAF13* locus.

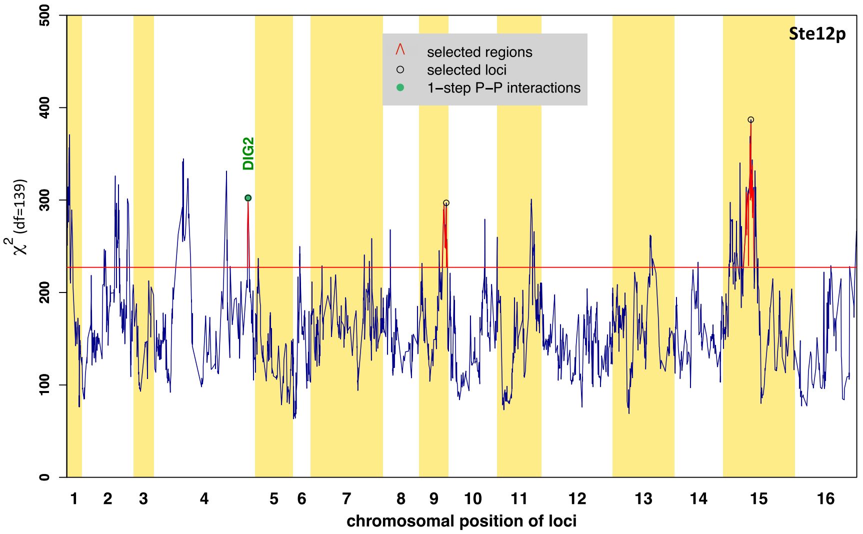

Fig. S6. χ^2 statistic profile obtained for Ste12p. Significant cQTL regions were detected using positive targets of Ste12p (139 genes). See Fig. S5 for annotation.

Table S1. Comparison of identified significant cQTL and aQTL for Gcn4p and Ste12p

TF	cQTL (this study)	aQTL (11)
Gcn4p	Chr4: 1,109,730–1,149,760 Chr13: 27,644–99,584 Chr16: 779,975–880,782	Chr2: 603,791–636,331
Ste12p	Chr4: 1,407,834–1,441,485 Chr9: 341,217–419,417 Chr15: 301,078–469,462	Chr8: 95,470–128,731

Table S2. Results from the β-galactosidase validation experiment

Time	RM 1	RM 2	RM 3	BY 1	BY 2	BY 3	BY DIG2(RM)1	BY DIG2(RM)2	BY DIG2(RM)3	RM DIG2(BY)1	RM DIG2(RM)2	RM DIG2(BY)3
No alpha-factor	642	719	861	3,707	3,673	3,546	1,855	1,757	1,834	716	771	789
0 min	775	736	785	4,520	4,558	4,318	2,592	2,539	2,519	637	705	667
15 min	756	777	786	20,132	19,500	19,571	17,690	17,767	17,864	792	776	751
30 min	1,194	1,221	1,215	17,693	19,107	19,795	32,337	33,057	31,159	672	759	726
60 min	2,293	2,373	2,506	21,096	24,116	25,185	15,863	18,007	18,264	739	693	701

Dataset S1. GO category enrichment analysis for inferred susceptibility signatures of seven selected TFs

Dataset S1